

Interpretation of some nuclear phenomena

Michael Tzoumpas

Mechanical and Electrical Engineer
National Technical University of Athens
Irinis 2, 15234 Athens, Greece

E-mail: m.tzoumpas@gmail.com

July 2021

Abstract. The stability of nickel nucleus ${}_{28}^{68}Ni$ compared to the ${}_{28}^{60}Ni$ and the instability of light nuclei with many neutrons are interpreted. Also, the elongation of heavy nuclei and the mechanism that acts as a catalyst for the nuclear fission of uranium ${}_{92}^{235}U$ are interpreted.

Keywords: Neutrons synod; beta decay β^- ; nuclear fission.

PACS numbers: 03.50.Kk, 12.10.-g

1. General Appearance

According to the unified theory^{1,2} of dynamic space the atomic nuclei^{3,4} have been structured through two fundamental phenomena.⁵ The inverse electric field⁶ of the proton and the electric entity of the macroscopically neutral neutron.⁷

The structure of the nuclei begins with the so-called lower-order nuclei, as the deuterium 2_1H , tritium 3_1H and helium 3_2He , which evolve into helium 4_2He ⁵ and then the first upper-order oxygen⁸ ${}^{16}_8O$, that has four nuclei 4_2He in a potential column of strong negative electric field as a follow:

Nitrogen nucleus⁹ ${}^{14}_7N$ is derived from one carbon¹⁰

$${}^{12}_6C = 3{}^4_2He \quad (1)$$

with addition of one deuterium 2_1H and so

$${}^{14}_7N = {}^{12}_6C + {}^2_1H = 3{}^4_2He + {}^2_1H \Rightarrow {}^{14}_7N = 3{}^4_2He + {}^2_1H. \quad (2)$$

Hence, oxygen nucleus⁸ ${}^{16}_8O$ is derived from ${}^{14}_7N$ (Eq. 2) by completing of the deuterium 2_1H as a helium 4_2He and so (Fig. 1)

$${}^{16}_8O = 3{}^4_2He + {}^4_2He \Rightarrow {}^{16}_8O = 4{}^4_2He. \quad (3)$$

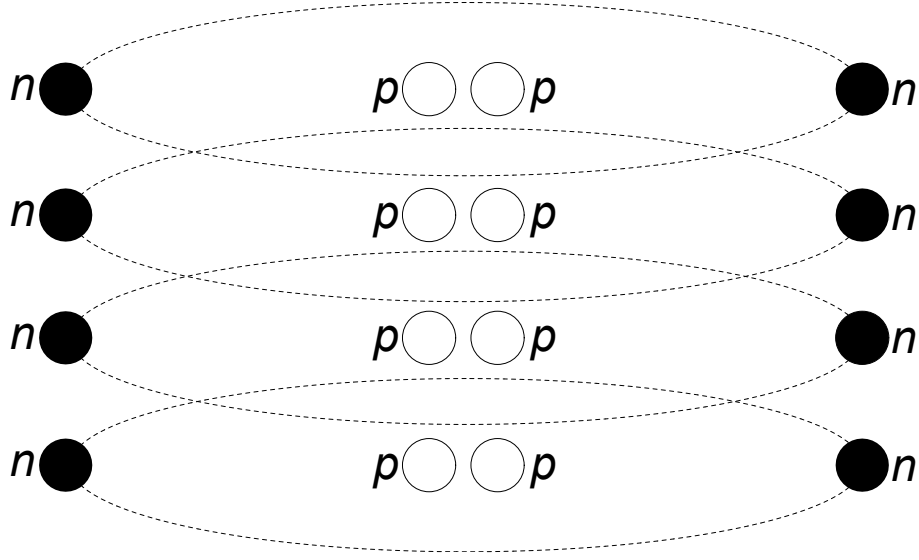


Figure 1. Structure model of oxygen ${}^{16}_8\text{O} = 4{}^4_2\text{He}$, as a column strong electric field of four coaxial helium nuclei ${}^4_2\text{He}$

After the helium nucleus ${}^4_2\text{He}$, the oxygen nucleus ${}^{16}_8\text{O}$ is the second stable one in Nature and the first upper-order nucleus.

So, the second upper-order calcium nucleus¹¹ ${}^{40}_{20}\text{Ca}$ (Fig. 2) is based on the fundamental natural phenomenon of mirror symmetry, by repetition of the first upper-order oxygen nucleus and one half of it, i.e. at the 2.5 factor

$${}^{40}_{20}\text{Ca} = {}^{16}_8\text{O} + \frac{1}{2} \cdot {}^{16}_8\text{O} + {}^{16}_8\text{O}. \quad (4)$$

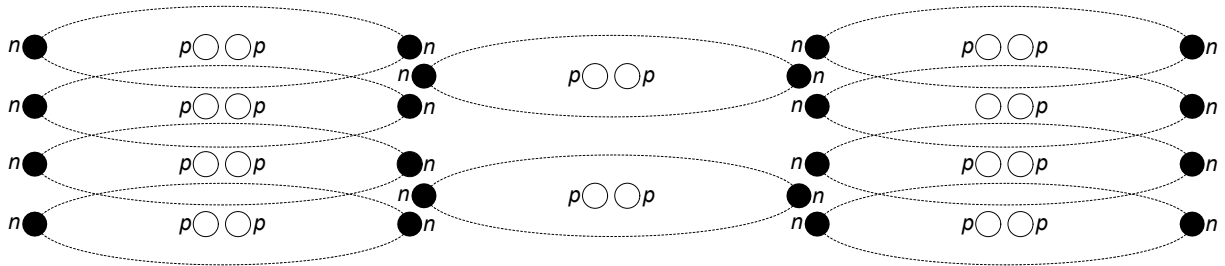


Figure 2. Structure model of calcium nucleus ${}^{40}_{20}\text{Ca} = {}^{16}_8\text{O} + \frac{1}{2} \cdot {}^{16}_8\text{O} + {}^{16}_8\text{O}$, as a mirror symmetry of two oxygen nuclei ${}^{16}_8\text{O}$ and two helium nuclei ${}^4_2\text{He}$ (one half oxygen), according to the 2.5 factor

The same stands with the third upper-order tin nucleus¹² ${}^{120}_{50}\text{Sn}$ (Figs 3, 4), which emerged from the second upper-order calcium ${}^{40}_{20}\text{Ca}$, according to the mirror symmetry and the same 2.5 factor plus 20 orbital bonding neutrons,¹³ i.e.

$${}^{120}_{50}\text{Sn} = {}^{40}_{20}\text{Ca} + \frac{1}{2} \cdot {}^{40}_{20}\text{Ca} + {}^{40}_{20}\text{Ca} + 20n. \quad (5)$$

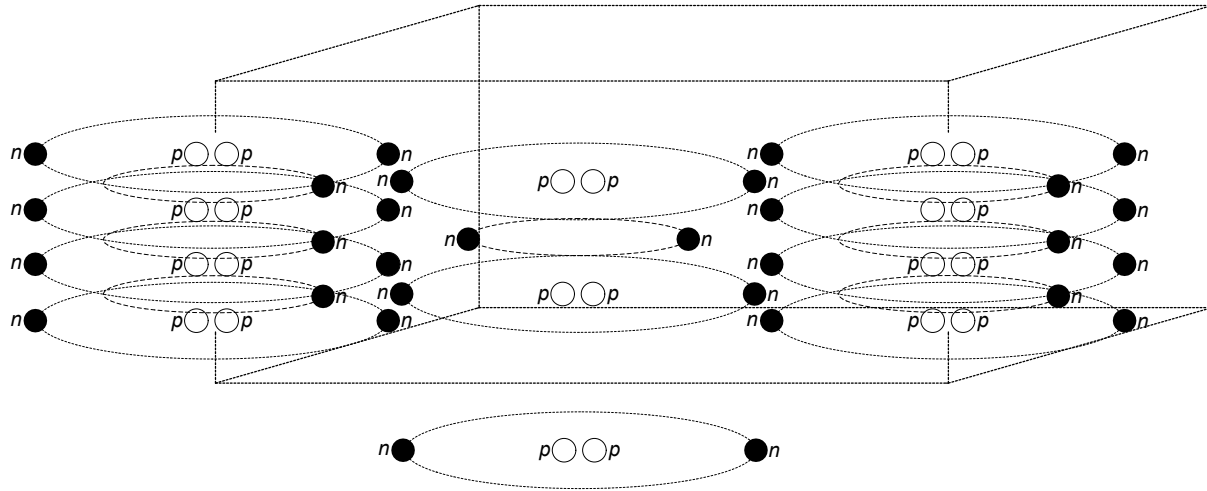


Figure 3. Stereoscopic representation of the tin nucleus ${}_{50}^{120}Sn$, where the same image on the other three sides of the rectangular parallelepiped is repeated, while the lonely helium nucleus ${}_{2}^4He$ is placed in its center

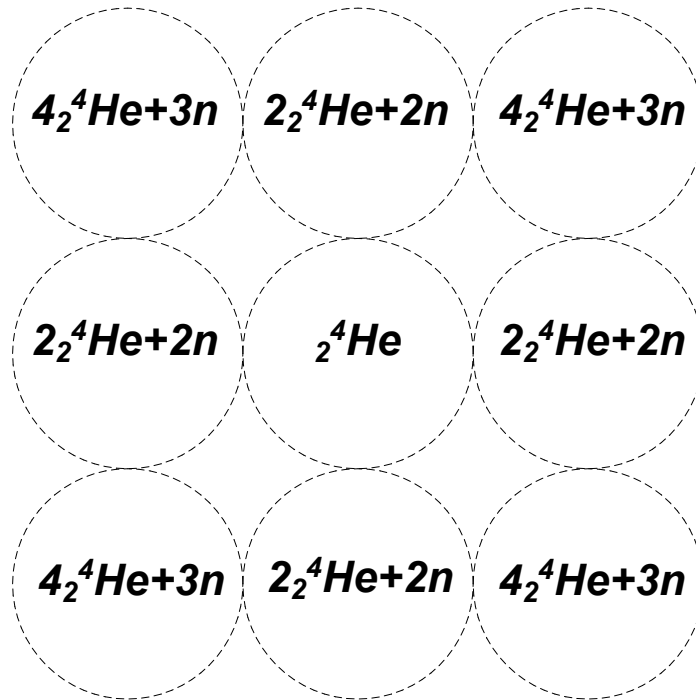


Figure 4. Top view of Fig. 3, where the mirror symmetry of the 2.5 factor for the construction of the tin nucleus ${}_{50}^{120}Sn$ appears

Additionally, the tin ${}_{50}^{120}Sn$ will further form the basis for the structure of all heavy nuclei up to the radioactive uranium ${}_{92}^{235}U$ (Fig. 11).

Specifically, rhenium nucleus ${}_{75}^{187}Re$

$${}_{75}^{187}Re = {}_{50}^{120}Sn + \frac{1}{2} \cdot {}_{50}^{120}Sn + 6n + n \quad (6)$$

is constructed by one tin ${}_{50}^{120}Sn$, one half of it and six orbital bonding neutrons are added, while one neutron added in deuterium 2_1H (one half helium 4_2He located in the center of tin ${}_{50}^{120}Sn$, Fig. 4) that evolves into tritium 3_1H (located in the center of $\frac{1}{2} \cdot {}_{50}^{120}Sn$, indicatively see Fig. 5).

So, bismuth nucleus ${}^{16}_83^{209}Bi$ (Fig. 5)



is constructed from the addition of four nuclei 4_2He and six orbital bonding neutrons adjacent to the corner potential column of rhenium ${}_{75}^{187}Re$ (Eq. 6).

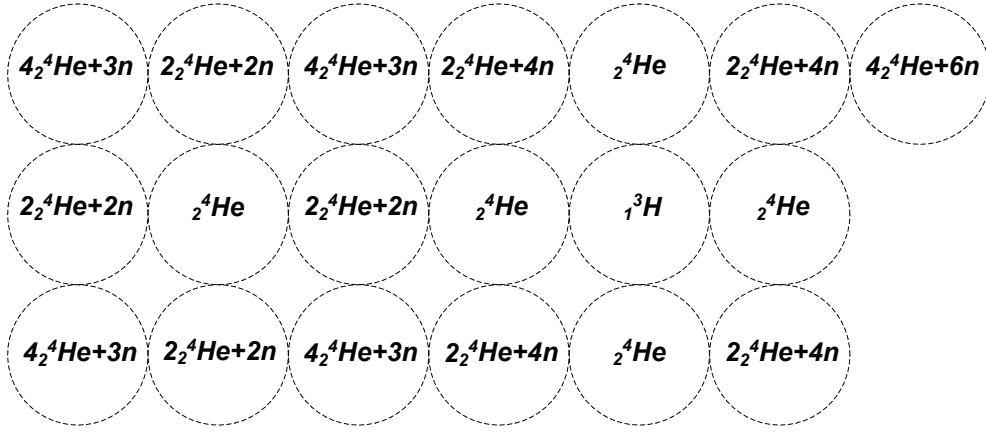


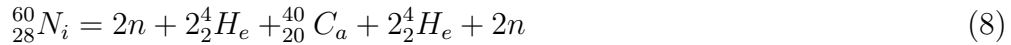
Figure 5. Representation of the bismuth nucleus ${}_{83}^{209}Bi$, where appears the addition of four helium nuclei 4_2He and six bonding neutrons adjacent to the corner potential column of rhenium nucleus ${}_{75}^{187}Re$

That is the simple and elegant structure model, according to which the nuclei consist of fixed nuclei 4_2He (plus deuterium 2_1H , tritium 3_1H and helium 3_2He , all evolving into helium 4_2He) and neutrons rotating around of them.

1.1. The stability of nickel nucleus ${}_{28}^{68}Ni$

The unexplained stability of the ${}_{28}^{68}Ni$ compared to ${}_{28}^{60}Ni$ is interpreted as follows:

Nickel nucleus ${}^{17}_28^{60}Ni$ (Fig. 6)



is derived by addition of two helium nuclei 4_2He right and left adjacent to a calcium nucleus ${}_{20}^{40}Ca$ (Fig. 2) as of two potential columns, while two orbital bonding neutrons at the above two potential columns are added, which reduce the strong negativity of the protons field and contribute to the stability of the nucleus.

However, nickel nucleus ${}^{17}_28^{68}Ni$ (Fig. 7)



have been constructed by addition of 8 orbital bonding neutrons to a ${}_{28}^{60}Ni$. These neutrons have been linked at the calcium nucleus during the tin ${}_{50}^{120}Sn$ (Figs 3, 4)

structure process. Therefore, the greater stability of the ${}^{68}_{28}Ni$, compared to the ${}^{60}_{28}Ni$, is due to its additional 8 neutrons.

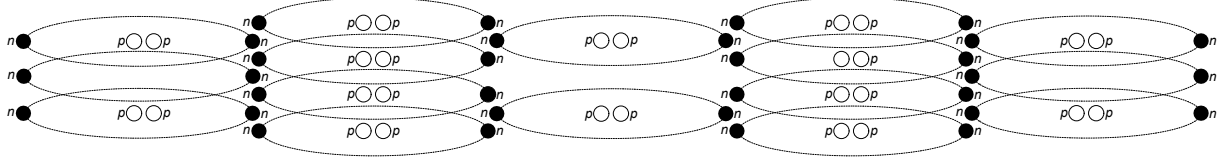


Figure 6. Structure model of nickel nucleus ${}^{60}_{28}Ni = {}^{40}_{20}Ca + 4{}^4_2He + 4n$, by addition of two helium nuclei 4_2He right and left adjacent to a calcium nucleus ${}^{40}_{20}Ca$ (Fig. 2) as of two potential columns, while four orbital bonding neutrons are added

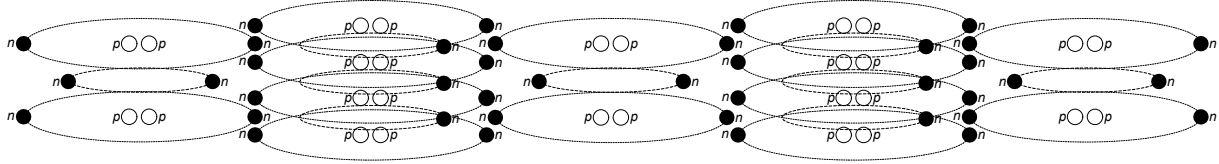


Figure 7. Structure model of nickel nucleus ${}^{68}_{28}Ni = {}^{60}_{28}Ni + 8n$, where the additional of 8 orbital bonding neutrons to a ${}^{60}_{28}Ni$ (Fig. 6). These neutrons have been linked at the calcium nucleus during the tin ${}^{120}_{50}Sn$ (Figs 3, 4) structure process

1.2. The instability of light nuclei with many neutrons

Oxygen nucleus ${}^{28}_8O$ (Fig. 8)

$${}^{28}_8O = {}^{16}_8O + 12n \quad (10)$$

is constructed from the addition of 12 orbital bonding neutrons, which are placed in orbits between the helium nuclei of the oxygen ${}^{16}_8O$ (Fig. 1). A beta decay β^- occur next, due to the frequent neutrons synod, making the oxygen nucleus ${}^{28}_8O$ unstable.

Magnesium nucleus ${}^{24}_{12}Mg$ (Fig. 9)

$${}^{24}_{12}Mg = {}^{16}_8O + 2{}^4_2He \quad (11)$$

is derived by addition of two helium nuclei 4_2He adjacent to an oxygen nucleus ${}^{16}_8O$.

However, magnesium nucleus ${}^{32}_{12}Mg$ (Fig. 10)

$${}^{32}_{12}Mg = {}^{24}_{12}Mg + 8n \quad (12)$$

is constructed from the addition of 8 orbital bonding neutrons, which are placed in orbits between the helium nuclei of the magnesium ${}^{24}_{12}Mg$ (Fig. 9). A beta decay β^- occur next, due to the frequent neutrons synod, making the ${}^{32}_{12}Mg$ with the many neutrons (i.e. 8 neutrons) greater unstable compared to the ${}^{24}_{12}Mg$.

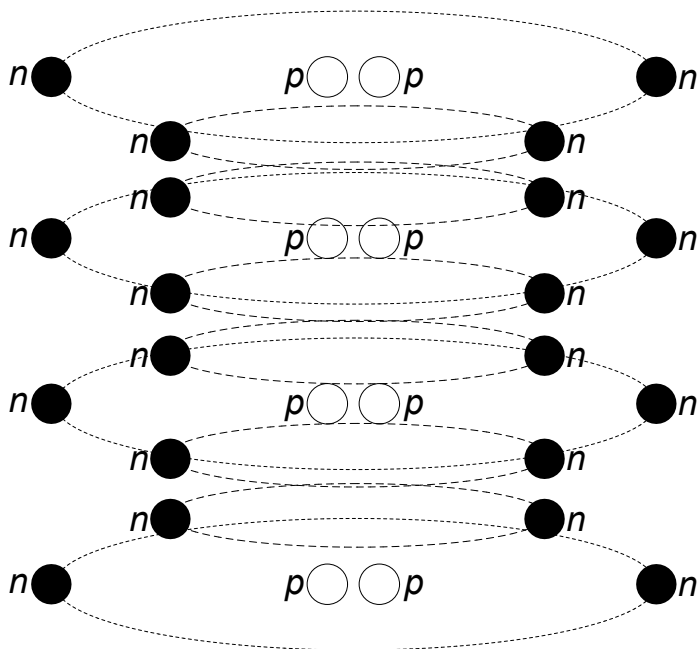


Figure 8. Structure model of oxygen ${}^{28}_8\text{O} = {}^{16}_8\text{O} + 12n$ by addition of 12 neutrons in orbits between the helium of the oxygen ${}^{16}_8\text{O}$ (Fig. 1)

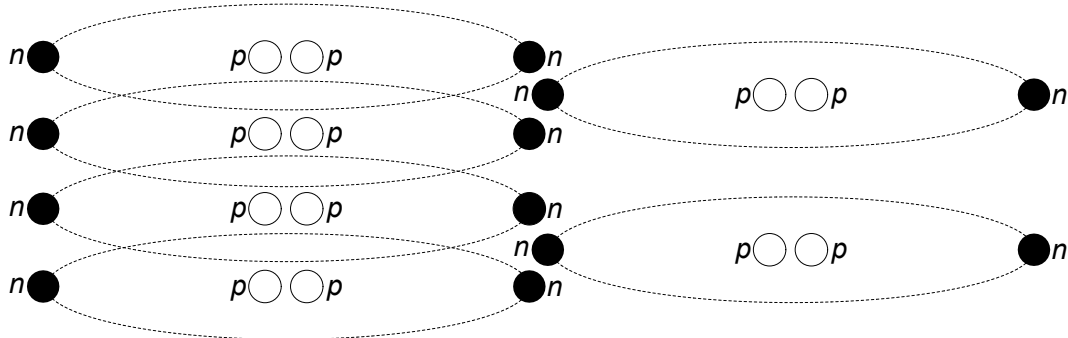


Figure 9. Structure model of magnesium nucleus ${}^{24}_{12}\text{Mg} = {}^{16}_8\text{O} + 2{}^4_2\text{He}$, with addition of two helium nuclei ${}^4_2\text{He}$ adjacent to an oxygen nucleus ${}^{16}_8\text{O}$

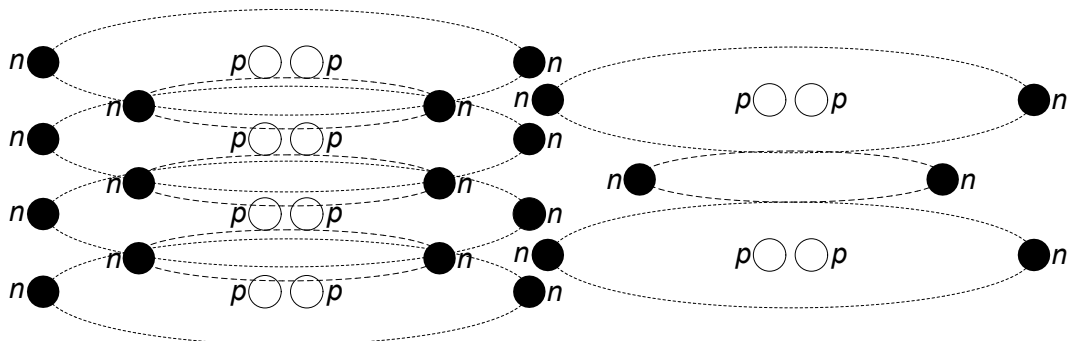


Figure 10. Structure model of magnesium nucleus ${}^{32}_{12}\text{Mg} = {}^{24}_{12}\text{Mg} + 8n$ with addition of 8 neutrons in orbits between the helium of the magnesium ${}^{24}_{12}\text{Mg}$ (Fig. 9)

1.3. The elongation of heavy nuclei

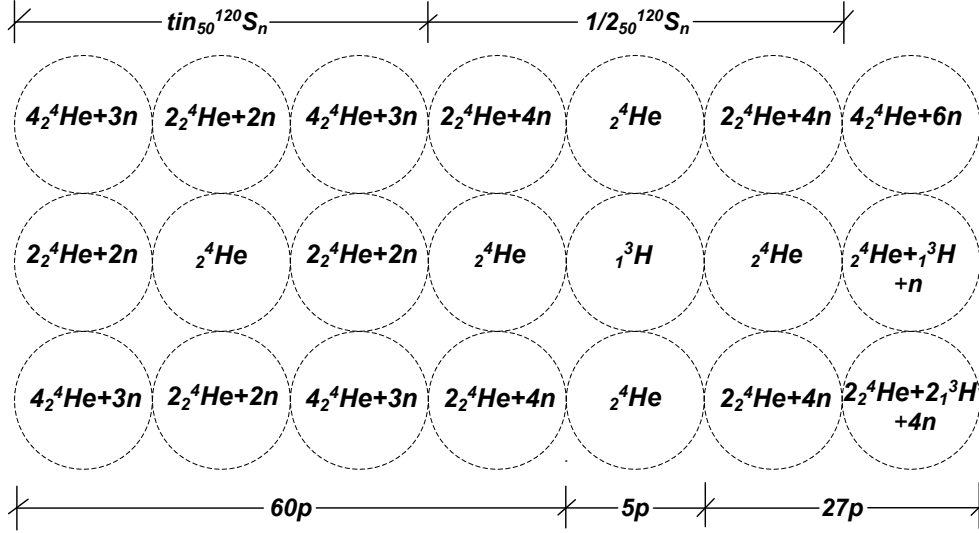


Figure 11. Representation of the uranium nucleus ${}_{92}^{235}\text{U}$, where appears the addition of one helium nucleus ${}^4_2\text{He}$, one tritium and one orbital bonding neutron at the middle potential column of bismuth nucleus ${}_{83}^{209}\text{Bi}$ (Fig. 5), while the addition of two helium nuclei ${}^4_2\text{He}$, two tritium nuclei and four orbital bonding neutrons appears at the other corner potential column of bismuth ${}_{83}^{209}\text{Bi}$. Also, the number and the distribution of protons determine the electrical potential and its isodynamic line that has a pear-shaped shape

Uranium nucleus¹³ ${}_{92}^{235}\text{U}$ (Fig. 11)

$${}_{92}^{235}\text{U} = {}_{83}^{209}\text{Bi} + ({}^4_2\text{He} + {}^3_1\text{H} + n) + (2{}^4_2\text{He} + 2{}^3_1\text{H} + 4n) \quad (13)$$

is constructed from the addition of one helium nucleus ${}^4_2\text{He}$, one tritium ${}^3_1\text{H}$ and one orbital bonding neutron adjacent to the middle potential column of bismuth nucleus¹⁶ ${}_{83}^{209}\text{Bi}$ (Fig. 5), while two helium nuclei ${}^4_2\text{He}$, two tritium nuclei ${}^3_1\text{H}$ and four orbital bonding neutrons are added at the other corner potential column of bismuth nucleus.

Figure 11 shows the number and the distribution of protons in the structure of the uranium nucleus ${}_{92}^{235}\text{U}$, which determine its electrical potential. In the first four rows of potential columns (tin ${}_{50}^{120}\text{Sn}$) there are 60 protons, in the last two rows (right) of potential columns there are 27 protons, while in the middle row of the connection unit ($\frac{1}{2} \cdot {}_{50}^{120}\text{Sn}$) there are only 5 protons. This distribution of protons creates 2 potential hills with an intermediate potential neck. The isodynamic line of this electrical potential has a pear-shaped shape.

Therefore, uranium nucleus ${}_{92}^{235}\text{U}$ (Fig. 11) is structured from helium nuclei ${}^4_2\text{He}$ (plus the tritium nuclei ${}^3_1\text{H}$), while the weak link of uranium ${}_{92}^{235}\text{U}$ is the unstable nucleus of the tritium ${}^3_1\text{H}$, which is located at the center of the above intermediate potential neck. This critical point becomes an attraction pole of neutrons, i.e. of a thermal neutron and rarely of a fast one, which it is cleaved (beta decay β^-), incorporating the produced proton into the tritium nucleus ${}^3_1\text{H}$, turning it into helium nucleus ${}^4_2\text{He}$. So,

this mechanism acts as a catalyst for the nuclear fission of uranium ${}_{92}^{235}\text{U}$ with the most common products being barium nucleus ${}_{56}^{141}\text{Ba}$ and the krypton nucleus ${}_{36}^{92}\text{Kr}$ plus three neutrons as in nuclear reaction



2. References

- [1] N.I.Gosdas, *The Unified Theory of Dynamic Space*, Greek Edition (Trohalia, Athens, 1999).
- [2] M.Tzoumpas, *Hubble's Law and antigravity - Higgs boson and gravity*, <http://viXra.org/abs/1710.0082> [Quantum Gravity and String Theory].
- [3] N.I.Gosdas, *The Structure of Nuclei* (chapter 4, pages 69-203), Greek Edition (SALTO, Thessaloniki, 2001).
- [4] M.Tzoumpas, *Structure model of atomic nuclei*, <http://viXra.org/abs/2001.0155> [Quantum Physics].
- [5] M.Tzoumpas, *Structure model of helium nucleus ${}^4_2\text{He}$* , <http://viXra.org/abs/2002.0340> [High Energy Particle Physics].
- [6] M.Tzoumpas, *Inverse electric-nuclear field*, <http://viXra.org/abs/1902.0266> (sections 1 and 2) [High Energy Particle Physics].
- [7] M.Tzoumpas, *Structure model of atomic nuclei*, <http://viXra.org/abs/2001.0155> (section 3) [Quantum Physics].
- [8] M.Tzoumpas, *Structure model of oxygen nucleus ${}^{16}_8\text{O}$* , <http://viXra.org/abs/2004.0145> [High Energy Particle Physics].
- [9] M.Tzoumpas, *Structure model of oxygen nucleus ${}^{16}_8\text{O}$* , <http://viXra.org/abs/2004.0145> (subsection 1.8) [High Energy Particle Physics].
- [10] M.Tzoumpas, *Structure model of oxygen nucleus ${}^{16}_8\text{O}$* , <http://viXra.org/abs/2004.0145> (subsection 1.7) [High Energy Particle Physics].
- [11] M.Tzoumpas, *Structure model of calcium nucleus ${}^{40}_{20}\text{Ca}$* , <http://viXra.org/abs/2004.0507> [High Energy Particle Physics].
- [12] M. Tzoumpas, *Structure model of tin nucleus ${}^{120}_{50}\text{Sn}$* , <http://viXra.org/abs/2005.0168> [High Energy Particle Physics].
- [13] M.Tzoumpas, *Structure model of oxygen nucleus ${}^{16}_8\text{O}$* , <http://viXra.org/abs/2004.0145> (subsection 1.2) [High Energy Particle Physics].
- [14] M. Tzoumpas, *Structure model of uranium nucleus ${}^{235}_{92}\text{U}$* , <http://viXra.org/abs/2006.0143> [High Energy Particle Physics].
- [15] M. Tzoumpas, *Structure model of uranium nucleus ${}^{235}_{92}\text{U}$* , <http://viXra.org/abs/2006.0143> (subsection 1.2) [High Energy Particle Physics].
- [16] M. Tzoumpas, *Structure model of uranium nucleus ${}^{235}_{92}\text{U}$* , <http://viXra.org/abs/2006.0143> (subsection 1.3) [High Energy Particle Physics].
- [17] M. Tzoumpas, *Structure model of tin nucleus ${}^{120}_{50}\text{Sn}$* , <http://viXra.org/abs/2005.0168> (subsection 1.2) [High Energy Particle Physics].
- [18] M.Tzoumpas, *Structure model of calcium nucleus ${}^{40}_{20}\text{Ca}$* , <http://viXra.org/abs/2004.0507> (subsection 1.2) [High Energy Particle Physics].